



## Numerical study of the plasticity effect on the behavior of short steel columns filled with concrete loaded axially

Yousria Boulmaali-Hacene Chaouche, Nadia Kouider, Kamel Djeghaba, Bachir Kebaili  
*Civil Engineering Laboratory (LGC), Badji Mokhtar- Annaba University, P. O. Box 12, 23000 Annaba, Algeria*  
*bc-yousria@hotmail.com; yousria.bchaouche@univ-annaba.dz*  
*nadia.kouider23@gmail.com; nadia.kouider@univ-annaba.dz*  
*kdjeghaba@gmail.com*  
*ba\_kebaili@hotmail.com*

**ABSTRACT.** For more than two decades, the construction technique using concrete filled steel tube (CFST) has been widespread throughout the world. Indeed, it has been demonstrated that the use of normal or high strength concrete, confined in a steel tube of circular shape can considerably improve its ductility as well as its load capacity, owing to the combination of the qualities of the two constituent materials; these tubes have an effortless execution, indeed, the concrete used in the CFST does not require formwork nor reinforcement, a durability of the two materials as well as a good behavior to fire, which was the effect desired at the origin of their elaboration. In this paper, we study the axial compression behavior of short circular steel tubes filled with concrete; their modelling will be performed using the ABAQUS/Standard calculation program. In order to accurately determine their behavior, we have created different models. Indeed, these tubes will be modeled in order to simulate different plastic state behaviours, namely a perfect elasto-plastic state, an elasto-plastic state with multilinear strain hardening and a third elasto-plastic behavior with strain hardening proposed by Tao et al. The tested columns consist of circular hollow sections which are designated in the literature as Concrete Filled Steel Tube (CFST), for which we vary the diameters, heights as well as the wall thicknesses, and which we fill with concrete of different qualities. The compressive behavior, including ultimate loads, confinement, load-deflection relationship and failure modes, was obtained from numerical models and compared with experimental and theoretical results based on Eurocode 4. All these results showed a good agreement and a satisfactory correlation, allowing us to assume that a correct modelling can be sufficient to simulate the behavior of CFST.

**KEYWORDS.** Concrete filled steel tubes; Axial compression; Finite element analysis; Confined concrete.



**Citation:** Boulmaali-Hacene Chaouche, Y., Kouider, N., Djeghaba, K., Kebaili, B., Numerical study of the plasticity effect on the behavior of short steel columns filled with concrete loaded axially, *Frattura ed Integrità Strutturale*, 62 (2022) 91-106

**Received:** 05.06.2022  
**Accepted:** 29.07.2022  
**Online first:** 08.08.2022  
**Published:** 01.10.2022

**Copyright:** © 2022 This is an open access article under the terms of the CC-BY 4.0, which permits unrestricted use, distribution, and reproduction in any medium, provided the original author and source are credited.



## INTRODUCTION

The advantages of steel elements are mainly the high tensile strength and ductility, while those of concrete elements are the compressive strength and stiffness which are important; that is why the combination of these two materials (steel and concrete), in the form of a composite structure provides the latter with an optimal combination of their respective qualities. The use of steel tubes filled with concrete began in the last century, this type of composite structures was used primarily to protect the metal sections from the adverse effects of fire, given their low resistance, but over time, researchers noticed that this type of elements had advantages that had not been taken into account at the beginning of their use from the 1960s; a few years later, a detailed study conducted by Tomii et al[1] on 268 composite columns (CFST) (Concrete Filled Steel Tube) demonstrated two modes of failure that were observed during the tests, namely global buckling for slender columns and concrete crushing accompanied by local buckling of the steel tube for short columns. The use of concrete-filled steel tubes in various construction areas is becoming a very attractive solution, not only because it increases the load capacity with a reduced cross-section, but also because it saves time and money during construction, and thus reduces costs significantly. Moreover, the use of normal or high strength concrete, confined in a steel tube of circular shape can significantly improve its ductility [2]; Indeed, many researchers have been interested in this type of mixed structures [3,4]. Also, the interest for their performances and the advantages they provide, increased, since the end of the 1990s; Indeed, it was found that the interaction between the concrete core confined by the steel tube of these composite elements also defined by (CFST) provided to the latter an increase in stiffness and resistance [2,3]; namely : facility of execution, good ductility, durability of both materials as well as good fire behavior, which was the expected effect at the origin of their elaboration; Indeed, the concrete used in the CFST does not require formwork or reinforcement, and its external surface is protected against any external aggression, the local buckling of the steel wall, due to the relatively small thickness of the wall, is delayed because it can occur in the concrete which can only deform outwards. Since then, several experimental and analytical studies have been conducted around the world. In the last decades [5–7], the finite element (FE) technique has become a more and more popular technique for modelling CFST columns due to the availability of commercially available software such as ABAQUS and ANSYS. FE analysis allows direct modelling of composite action between steel and concrete components, and various factors, such as local and global imperfections and boundary conditions, can be considered more accurately; also all these investigations have resulted in the development of different regulations related to different countries such as Australia, China, Japan, USA (ACI) and European countries (Eurocode4)[8–11]. Although this type of columns may be suitable for high-rise buildings in high seismic regions, their use has been limited due to a lack of information on the true strength and nonlinear behavior of the elements composing them, namely the steel tube and the concrete that it is in-filled. Indeed, many researchers have been interested in this type of mixed structures of circular shape including[10–13] while others have been interested in steel tubes of different shapes(rectangular, oval...) [4,10,14,15].

All these experimental and numerical studies have been conducted for nearly four decades, in fact the numerical calculation is widely required for the modelling of structures, and the Finite Element Method is the most used for the modelling of all types of structures, and more recently, many authors continue to be interested until today in this type of composite structure by adopting different approaches from those previously recommended and in particular the type of composite we are interested in ,namely ,steel tubes filled with concrete or CFST and this with the help of calculation programs such as ABAQUS[13,16], thus considerably reducing the computational time, and in addition leading to a considerable decrease in the cost of these researches, which previously required very expensive laboratory experiments. All these works pushed us to be interested in our turn in this type of composite structures (CFST), following their use in constant evolution, as well as their behavior intimately related to the constitutive laws of the materials used, in particular that of the concrete confined according to the instructions of the Eurocode 4[8]; moreover we will suppose that the effect of the confinement is non-existent at the beginning of loading, and would intervene only late, at the time of the lateral expansion and the transfer of load from the steel tube to the concrete. For a steel tube filled with concrete (CFST), under axial compression, the concrete core expands laterally and is confined by the steel tube. This confinement would be passive in nature and could improve the strength and ductility of the concrete. We assume that the confined concrete is in a triaxial stress state [11], and that the steel is in a biaxial state after the interaction between the two components has occurred.

Finite element analysis is a method that is being increasingly used because it allows taking into account the composite action providing that a rational and accurate concrete model is available to describe the behavior of concrete under passive confinement.



This observation led us to study the different laws of behavior of steel perfect elasto-plasticity, elasto-plasticity with multilinear strain hardening and elasto-plasticity with strain hardening proposed by Tao et al [12], for which we studied a number of models for which we varied some geometric and physical characteristics in order to highlight the behavior and the evolution of the results obtained during our simulations

### THEORETICAL ASPECT

In order to describe, with more or less accuracy, the behavior in nonlinear analysis of an element or a structure, related to the transition from an elastic state to an elasto-plastic state, it is necessary to study these phenomena from the theoretical point of view. Indeed, different "stress-strain" curves ( $\sigma - \epsilon$ ) representative of the behavior of the models, which recommended by many researchers, have been used for the steel material.

The first model is that of the steel with perfect elasto-plastic behavior represented by Fig. 1-a, for which the hardening of the material is neglected in order to simplify the analytical resolution of the problems inherent to the plasticity of the materials, for this model  $E_s$  is the elasticity modulus of the used steel. The second one represents the elasto-plastic behavior with multilinear hardening, which takes into account the hardening of the material due to its ductility and therefore is closer to reality Fig. 1-b.

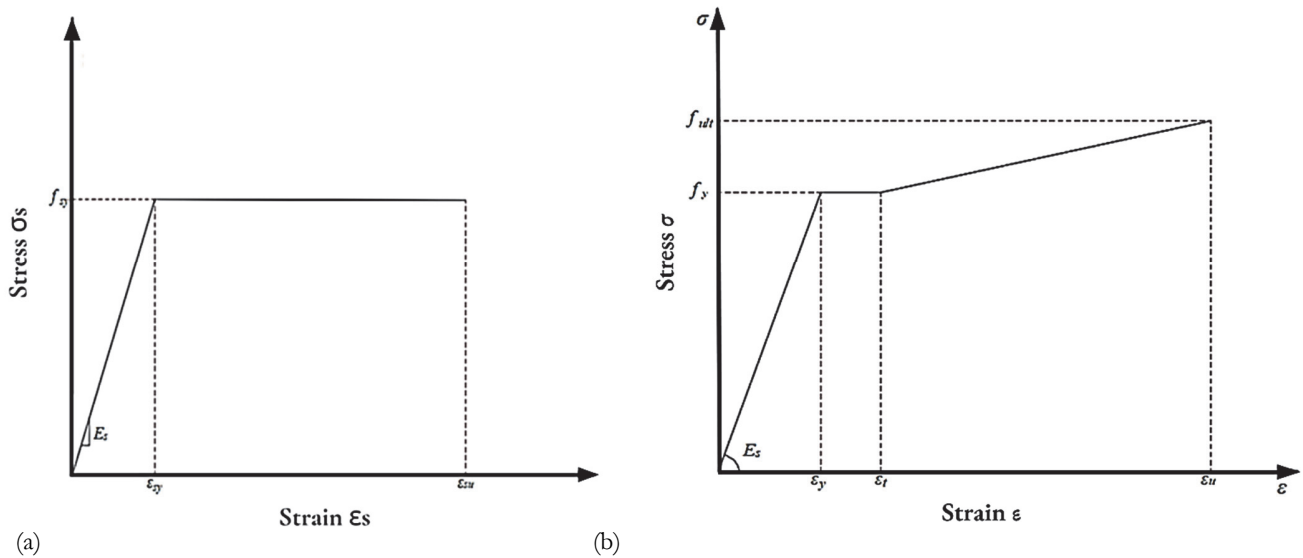


Figure 1: Stress-strain relation for steel tube (a) Perfect elasto-plastic, (b) Elasto-plastic with multi-linear hardening [5].

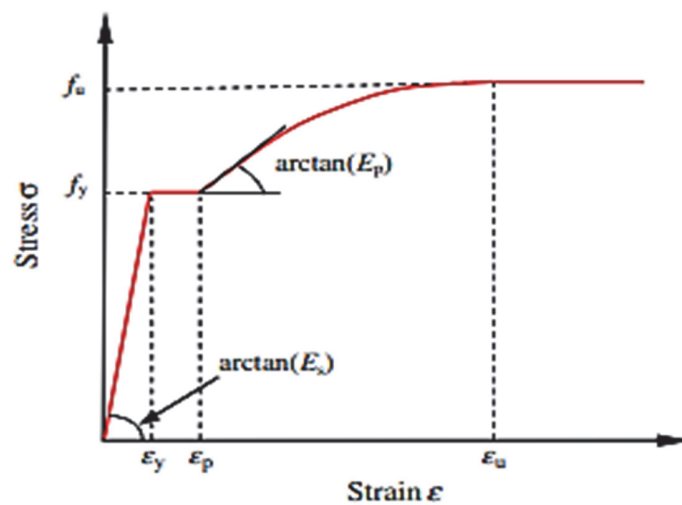


Figure 2: Stress-Strain ( $\sigma - \epsilon$ ) model proposed by Tao et al. for structural steel [12].

The third model, is represented by a steel behavior law proposed by Tao et al [12] (Fig. 2). The  $\sigma - \varepsilon$  curve determining this type of steel, is given by the model that was proposed by Tao et al [12] for structural steel with  $f_y$  value varying from 200 MPa to 800 MPa. This model was used to simulate the steel for CFST circular columns, which are calculated as follows:

$$\sigma = \begin{cases} E_s \varepsilon & 0 \leq \varepsilon \leq \varepsilon_y \\ f_y & \varepsilon_y \leq \varepsilon \leq \varepsilon_p \\ f_u - (f_u - f_y) \left( \frac{\varepsilon_u - \varepsilon}{\varepsilon_u - \varepsilon_p} \right)^p & \varepsilon_p \leq \varepsilon \leq \varepsilon_u \\ f_u & \varepsilon \geq \varepsilon_u \end{cases} \quad (1)$$

where  $f_u$  is the ultimate strength;  $\varepsilon_y$  is the yield strain,  $\varepsilon_y = f_y / E_s$ ;  $\varepsilon_p$  is the strain at the onset of strain hardening;  $\varepsilon_u$  is the ultimate strain corresponding to the ultimate strength,  $p$  is the strain-hardening exponent, which can be determined by:

$$p = E_p \left( \frac{\varepsilon_u - \varepsilon_p}{f_u - f_y} \right) \quad (2)$$

where  $E_p$  is the initial modulus of elasticity at the beginning of strain-hardening and can be taken to be equal to  $0.02 E_s$ ,  $\varepsilon_p$  and  $\varepsilon_u$  are determined using the equations below:

$$\varepsilon_p = \begin{cases} 15\varepsilon_y & f_y \leq 300 \text{ MPa} \\ \left[ 15 - 0.018(f_y - 300) \right] \varepsilon_y & 300 \text{ MPa} < f_y \leq 800 \text{ MPa} \end{cases} \quad (3)$$

$$\varepsilon_u = \begin{cases} 100\varepsilon_y & f_y \leq 300 \text{ MPa} \\ \left[ 15 - 0.015(f_y - 300) \right] \varepsilon_y & 300 \text{ MPa} < f_y \leq 800 \text{ MPa} \end{cases} \quad (4)$$

In Fig. 2 only three parameters, yield strength ( $f_y$ ), ultimate strength ( $f_u$ ), and elastic modulus ( $E_s$ ), are required to determine the complete stress-strain curve. The value of  $E_s$  is equal to 210,000 MPa for the model developed in the following. Similarly, the following equation proposed by Tao et al [12] was used to determine  $f_u$  from  $f_y$ :

$$f_u = \begin{cases} \left[ 1.6 - 2 \cdot 10^{-3} (f_y - 200) \right] f_y & 200 \text{ MPa} \leq f_y \leq 400 \text{ MPa} \\ \left[ 1.2 - 3.75 \cdot 10^{-4} (f_y - 400) \right] f_y & 400 \text{ MPa} \leq f_y \leq 800 \text{ MPa} \end{cases} \quad (5)$$

For the infill material which is concrete, we rely on the recommendations of Eurocode 4, as well as those proposed by Mander et al [17], to describe the behavior of confined concrete. The stress-strain relationship of unconfined concrete is shown in (Fig.3), where  $f_{ck}$  is the cylindrical compressive strength of concrete ( $f_{ck} = 0.8 f_{ck,cub}$  and  $f_{ck,cub}$  is the cubic compressive strength of concrete).  $\varepsilon_{ck}$  is the strain corresponding to  $f_{ck}$ ; for unconfined concrete,  $\varepsilon_{ck}$  can be taken



equal to according to Eurocode 4 [8]. The stress-strain relationship of confined concrete can be deduced from the characteristic parameters of unconfined concrete with confining conditions. The stress-strain curve of confined concrete is shown in the (Fig.3). For concrete confined by circular steel tube sections, the maximum strength  $f_{cc}$  and the corresponding strain  $\varepsilon_{cc}$  [17–19].

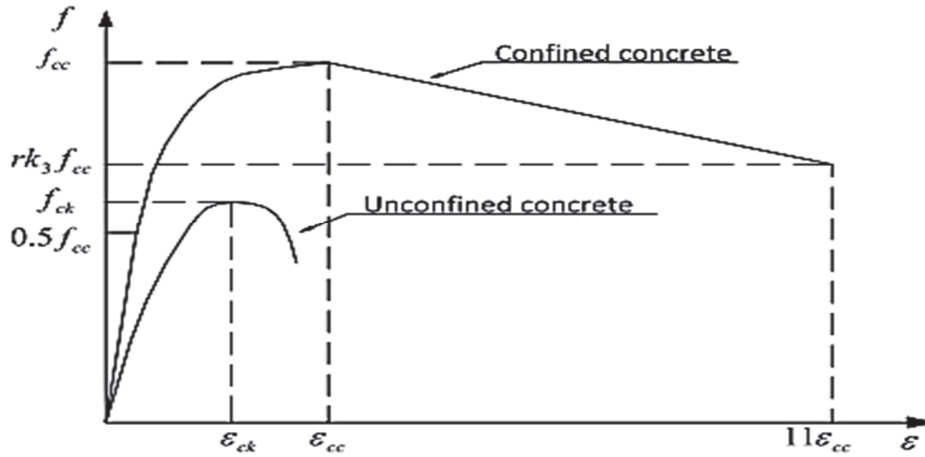


Figure 3: Stress-strain curves of concrete unconfined and confined by circular hollow sections [17].

In order to simulate the axial compression behavior of tubular steel sections filled with concrete with circular cross-sections and according to the studies of Richart et al [20], the calculation formulas are as follows:

$$f_{cc} = f_{ck} + k_1 f_1 \tag{6}$$

$$\varepsilon_{cc} = \varepsilon_{ck} \left( 1 + k_2 \frac{f_1}{f_{ck}} \right) \tag{7}$$

For which the values of  $k_1$  and  $k_2$  are 4.1 and 20.5 respectively. For circular steel columns filled with concrete, B. Kebaili [11] proposed that the values of  $f_1$  be determined by the following relationship:

$$f_1 = 2 \cdot \frac{t}{D} \cdot (0.578 \cdot f_y) \quad \text{for} \quad 21.7 \leq \frac{D}{t} \leq 47 \tag{8}$$

where:

$D$  = external diameter of the tube section;

$t$  = wall thickness of the steel tube;

$f_y$  = yield strength of the steel section.

The stress-strain curve of confined concrete, as shown in Fig.3 is expressed in three parts. The first part defines the linear property of confined concrete and the proportional limit stress can be assumed to be equal to  $0.5f_{cc}$ . The initial Young's modulus of the confined concrete is calculated from the empirical formulation given by EC4 and calculated from the formula  $E_{cc} = 22000(f_{cc} / 10)^{0.3}$ . The Poisson's ratio of the confined concrete has the value (0.2). The second part of the stress-strain curve describes the non-linear part, before the concrete reaches its maximum strength, from the proportional limit stress  $0.5f_{cc}$  to the maximum strength of the confined concrete  $f_{cc}$ . This part is given as follows:



$$f = \frac{E_{\alpha} \varepsilon}{1 + (R + R_E - 2) \left( \frac{\varepsilon}{\varepsilon_{\alpha}} \right) - (2R - 1) \left( \frac{\varepsilon}{\varepsilon_{\alpha}} \right)^2 + R \left( \frac{\varepsilon}{\varepsilon_{\alpha}} \right)^3} \quad (9)$$

where:

$$R_E = \frac{E_{\alpha} \varepsilon_{\alpha}}{f_{\alpha}}, \quad R = \frac{R_E (R_{\sigma} - 1)}{(R_E - 1)^2} - \frac{1}{R}, \quad R_{\sigma} = R_{\varepsilon} = 4$$

The third part of the curve starts from the maximum strength of the confined concrete  $f_{\alpha}$  and ends at the ultimate value of the strength  $f_u = r k_3 f_{\alpha}$  to which an ultimate value of the strain  $\varepsilon_u = 11 \varepsilon_{\alpha}$  corresponds. For circular steel tube sections filled with concrete with  $21.7 \leq D/t \leq 150$ , Hu et al [21] proposed the following values of parameter  $k_3$ :

$$K_3 = 1 \quad \text{for} \quad 21.7 \leq D/t \leq 40$$

$$k_3 = 0.0000339 \left( \frac{D}{t} \right)^2 - 0.0100085 \left( \frac{D}{t} + 1.3491 \right) \quad \text{for} \quad 40 \leq D/t \leq 150$$

Based on the experimental studies [3,18] conducted that the parameter  $r$  can be taken equal to 1.0 for concrete with cubic strength of 30 MPa and 0.5 for concrete with strength of 100 MPa, respectively, and linear interpolation can be used for concrete with cubic compressive strength between 30 and 100 MPa.

## FINITE ELEMENT MODELLING

The finite element method is a numerical analysis technique for obtaining approximate solutions to a wide variety of engineering problems. The basic concept of finite element analysis is that a structure is divided into a finite number of elements with finite dimensions, reducing the infinite degrees of freedom of the structure to finite degrees of freedom [18]. There is no doubt that large-scale physical tests provide a better understanding of the behavior of structural elements, but these are costly and time-consuming, and it is also fastidious to perform extensive parametric studies exclusively through experimental testing, which encourages the use and development of numerical modelling in engineering research. Many numerical models [11–13] have been proposed to predict the behavior of concrete-filled steel tubes following the increasing use of composite columns in modern buildings.

The various experiments have shown that the failure modes of concrete-filled steel tubes under axial compressive loads are characterized by localized buckling of the hollow sections and cracking of the concrete, which differ from thin concrete-filled tubular columns under axial compression whose failure mode is generally global buckling because they are more slender. This observation leads us to suppose that the behavior in axial compression of short columns filled with concrete could depend on the material properties of the constituent elements and their combined actions, which led us to the development of different models (T1C1.....T3C3, where T represents the steel tube and C the concrete with which it is filled) whose numerical modelling was conducted on the code of calculation by finite elements ABAQUS.

The geometrical and mechanical characteristics of the steel tubes filled with concrete are presented in Tab. 1 and Fig. 4. A Poisson's ratio equal to 0.2 was adopted for concrete and 0.3 for steel (Tab. 2). The three steel pipes are of class 1 according to the instructions of Eurocode 3 [22], for which three behavior laws were used, namely: perfect elasto-plastic behavior, elasto-plastic behavior with multilinear strain hardening and elasto-plastic behavior with strain hardening proposed by Tao et al [12].

The concrete filled tubes are subjected to axial compressive loading which leads to a dominant compressive deformation in the concrete core without rotation. Therefore a three-dimensional 8-node solid element would be the most appropriate type of element to use to reflect the deformation characteristics of the concrete[5–7,23]. Each component was modelled as an independent part, the steel tube and the concrete were modelled using the 8-node reduced integration linear brick element "C3D8R" available in the ABAQUS library [23] (Fig. 5). This brick element can be effectively used in material



nonlinear analysis, including plasticity, contact, large displacement, and ruin, furthermore, the use of small three-dimensional eight-node solid elements for the steel section not only reasonably tracks the contact area, but also, reflects the deformation characteristics of the hollow section. To be consistent and close to a real setup and to avoid local instability effects during loading, two rigid plates were modelled to simulate the uniformity of loading on the CFST composite (steel tube filled with concrete) [10].

Models	D (mm)	t (mm)	D/t	H/D	$f_e$ (MPa)	$f_c$ (MPa)
T1C1	70	3	22,33	3	240	15
T1C2	70	3	22,33	3	310	25
T1C3	70	3	22,33	3	310	32
T2C1	87	2,5	33,80	3	240	15
T2C2	87	2,5	33,80	3	310	25
T2C3	87	2,5	33,80	3	310	32
T3C1	105	2,5	41,00	3	240	15
T3C2	105	2,5	41,00	3	310	25
T3C3	105	2,5	41,00	3	310	32

Table 1: Characteristics of the steel tubes studied.

Element	Elastic limit $f_{yb}$ (MPa)	Density $\gamma$ (kg/m <sup>3</sup> )	Young's modulus E(MPa)	Poisson Coefficient $\nu$
Steel tubes	240	7850	210000	0.3
	310			

Table 2: Mechanical properties of steel tubes studied.

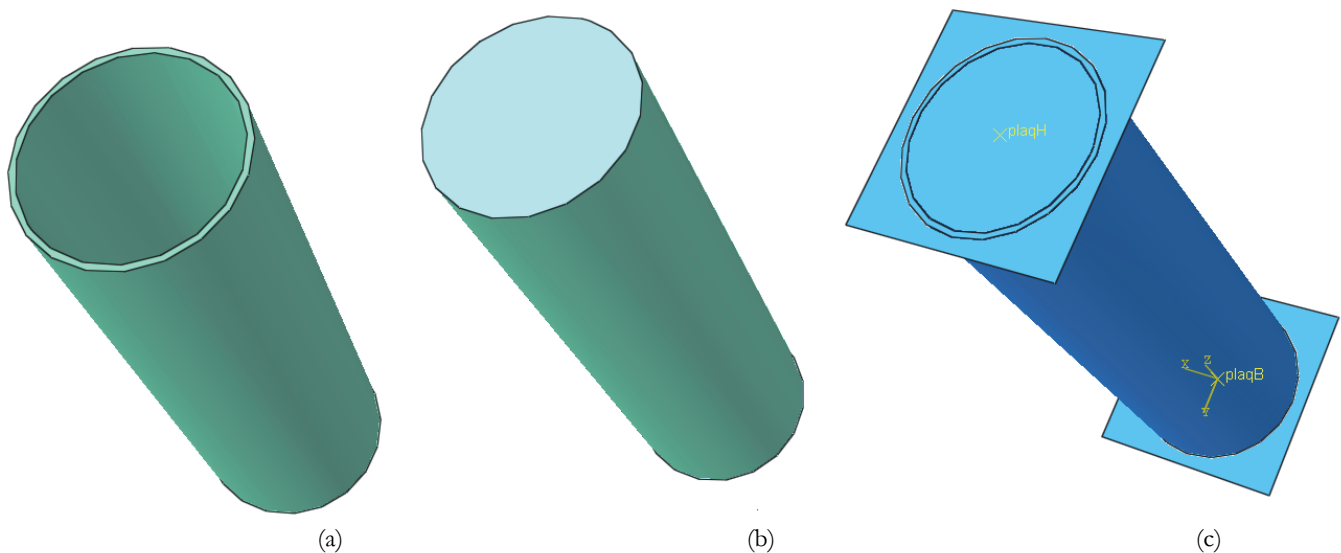


Figure 4: Presentation of the model adopted for the numerical simulation, (a) Empty steel tube, (b) concrete core, and (c) concrete filled tube.

For the Finite Element model, there is direct contact between the extremity plates and the extremity surfaces of the short column, so a contact function available in the ABAQUS calculation software was used to simulate the interaction between the rigid plate and the extremity surface of the column. The contact was defined as a «surface-to-surface» contact with a «finite sliding» contact. The «hard contact» option defines the contact in the normal direction and a high friction ('rough' option) was applied for the contact behavior in the tangential direction (Fig.6). Concerning the interaction between the



contacting surfaces of the steel tube and the concrete core (inner surface of the steel tube and outer surface of the concrete cylinder), we have defined it by a tangential contact materialized by a friction coefficient equal to 0.2 (Fig. 6a). For the Finite Element model, the lower rigid plate, in contact with the bottom of the steel tube, is fixed in all six directions ( $U_x=U_y=U_z=0, \theta_x=\theta_y=\theta_z=0$ ) and the upper rigid plate is fixed in all five directions except the vertical displacement direction ( $U_x=U_y=0, \theta_x=\theta_y=\theta_z=0$ ). The models are subjected to axial center compression loading represented by an imposed displacement applied to the upper rigid plate (imposed displacement  $U_z=10\text{mm}$ ) (Fig. 6b).

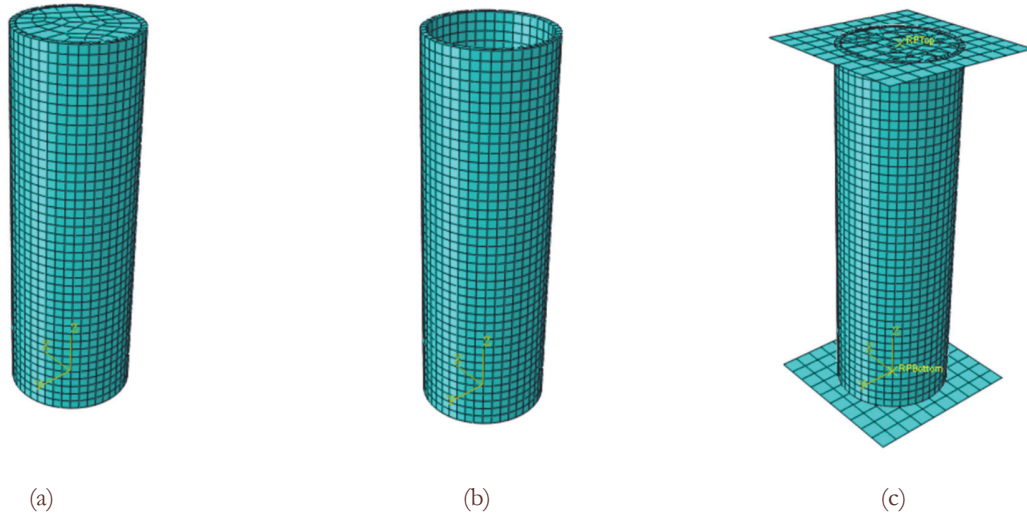


Figure 5: Mesh of columns filled with rigid plates at the ends: (a) Concrete, (b) Steel tube, (c) Tube filled with concrete.

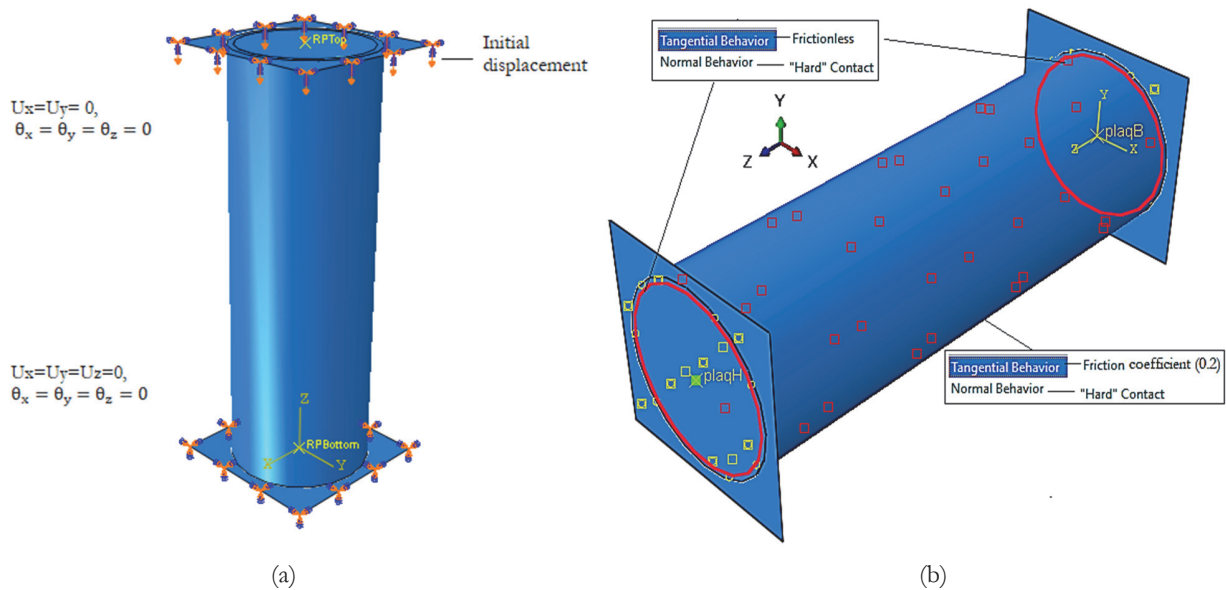


Figure 6: Interaction loading and limit conditions of the models (a) Loading and boundary conditions, (b) interaction contact.



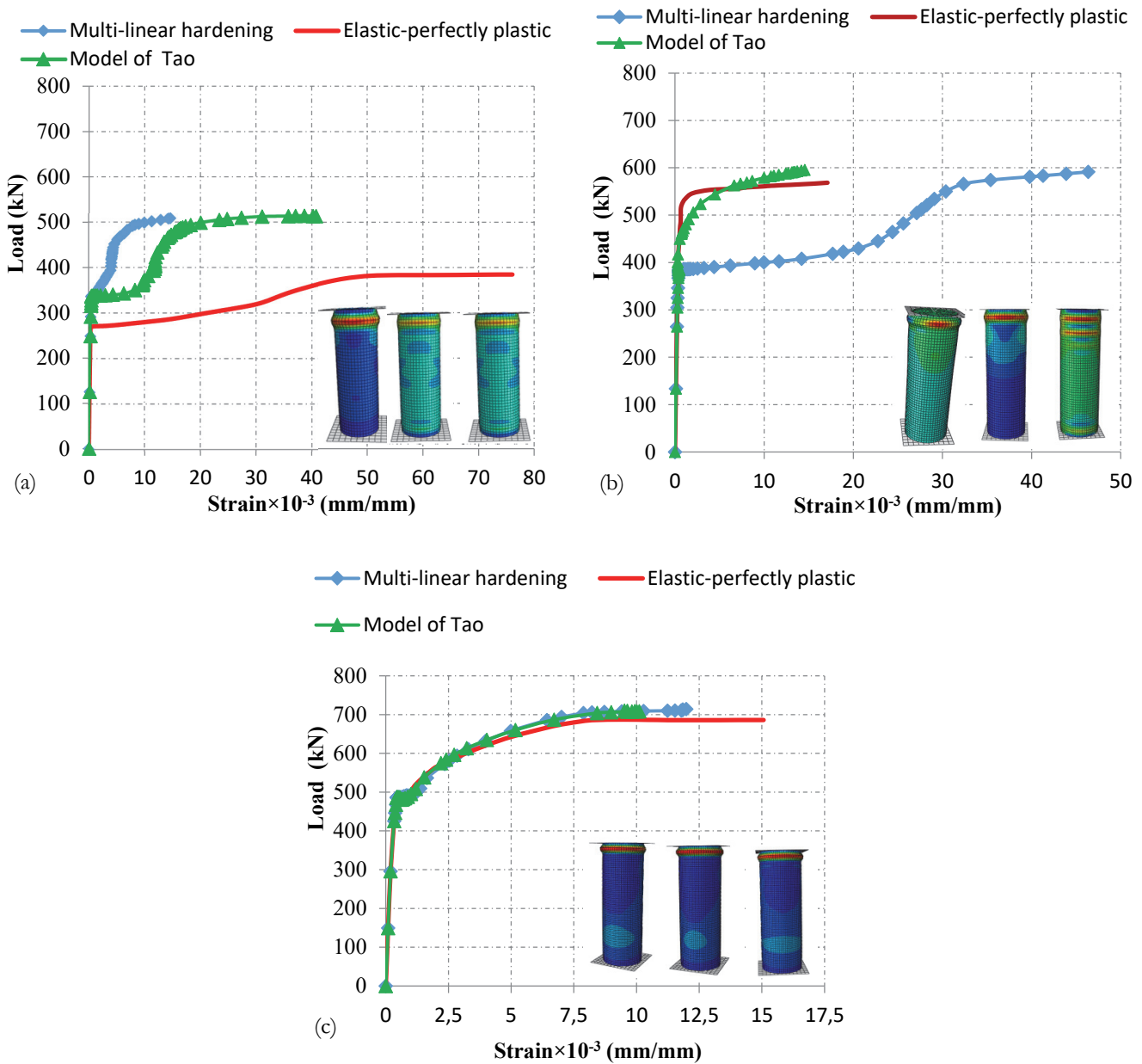


Figure 7: Lateral load-deformation state under different plastic state behaviours:(a) Tube T1C1, (b) Tube T2C1, (c) Tube T3C1.

## RESULTS AND DISCUSSION

Concerning the three short tubes T1C1, T2C1 and T3C1, whose mechanical characteristics of the two materials steel and concrete are identical, the numerical results of the load-deformation state measured at the level of the median section of the tube, followed an elasto-plastic behavior (material nonlinearity), characterized by a local buckling such as described by several authors of which Cheng Fang et al [14].

T1C1 tube: the curves of the three load-deformation states for the different behaviours are almost merged, however, Tao's model presents large tensile strains reaching a positive value of  $35 \times 10^{-3}$ , unlike that of the other two behaviours namely multi-linear hardening and perfectly plastic (Fig. 7a). Based on the theory proposed by Tao et al [12], we notice that increasing the diameter of the steel tube by 20% (T2C1) and 33% (T3C1) leads to a significant decrease in the strain

by 65% and 71% respectively (Figs. 7b and 7c). The concrete core and the steel tube can experience different deformations, but the confinement of the concrete and the action of the bond on their contact surface will produce positive effects (deformation reduction).

For the perfectly plastic model, the increase of the tube diameter leads to a plastic flow of the steel, resulting in an increase of the deformations respectively of 69% and 71% for T2C1 and T3C1 because these models neglect the work hardening of the material.

The perfect elasto-plastic model is mainly used from an academic point of view to simplify the analytical solution of the problems that occur during the transition from an elastic to a plastic state.

Finally, for the model with linear strain hardening, the maximum deformation decreases by 35% and 38% for T2C1 and T3C1 respectively, compared to T1C1 (Fig. 7).

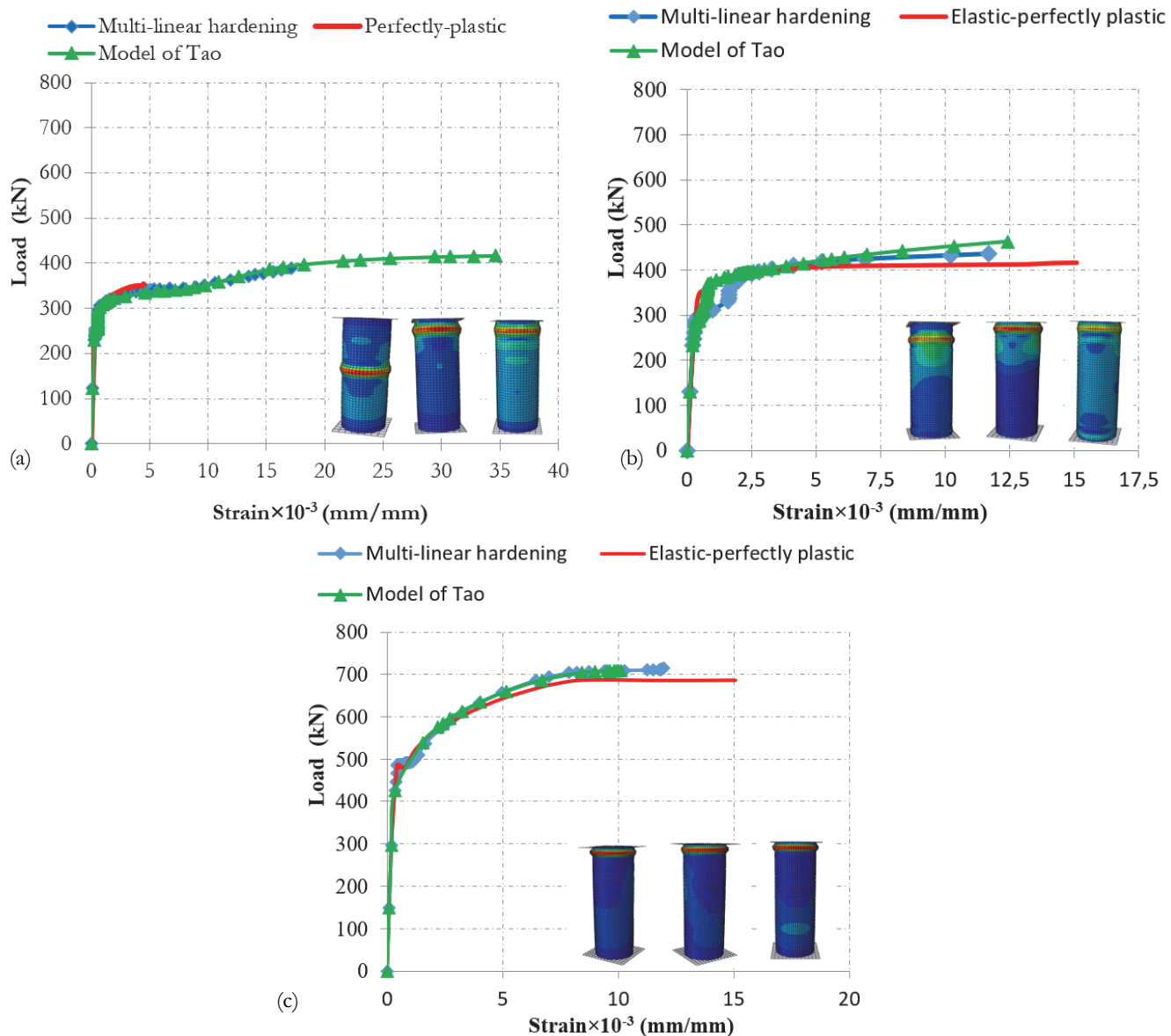


Figure 8: Lateral load-deformation state under different plastic state behaviours (a) Tube T1C2, (b) Tube T2C2, (c) Tube T3C2.

By varying the constitutive laws, the T1C2 tube, whose behavior in an elastoplastic state with multilinear work hardening, presents a difference characterized by localized buckling in the middle section of the tube (Fig. 8a), in comparison with the two others for which it is located at the top of the tube (Figs. 8b and 8c). In general, the curves follow a non-linear pace with an improvement in the deformations linked to that of the quality of the concrete, and to the resistance of the



steel; a decrease of around 42% for the T2C2 tube and 80% for the T3C2 tube compared to the T1C2 tube. For the T3C2 tube (Fig. 8c), we find that the resulting curves are confused, which proves that the variation of the plasticity behavior laws does not significantly influence the behavior of the model. We also observe that the T2C2 and T3C2 tubes resist the failure load much better than the T1C2 tube (Figs. 8a, 8b and 8c).

All three tubes show local buckling at the load application area. For the model proposed by Tao et al [12], the increase in the diameter of the tube over 20% has no influence on its behavior, from the point of view of deformation, which presents a reduction around 60% for the T2C3 and T3C3 tubes in comparison with the T1C3 tube (Fig. 9).

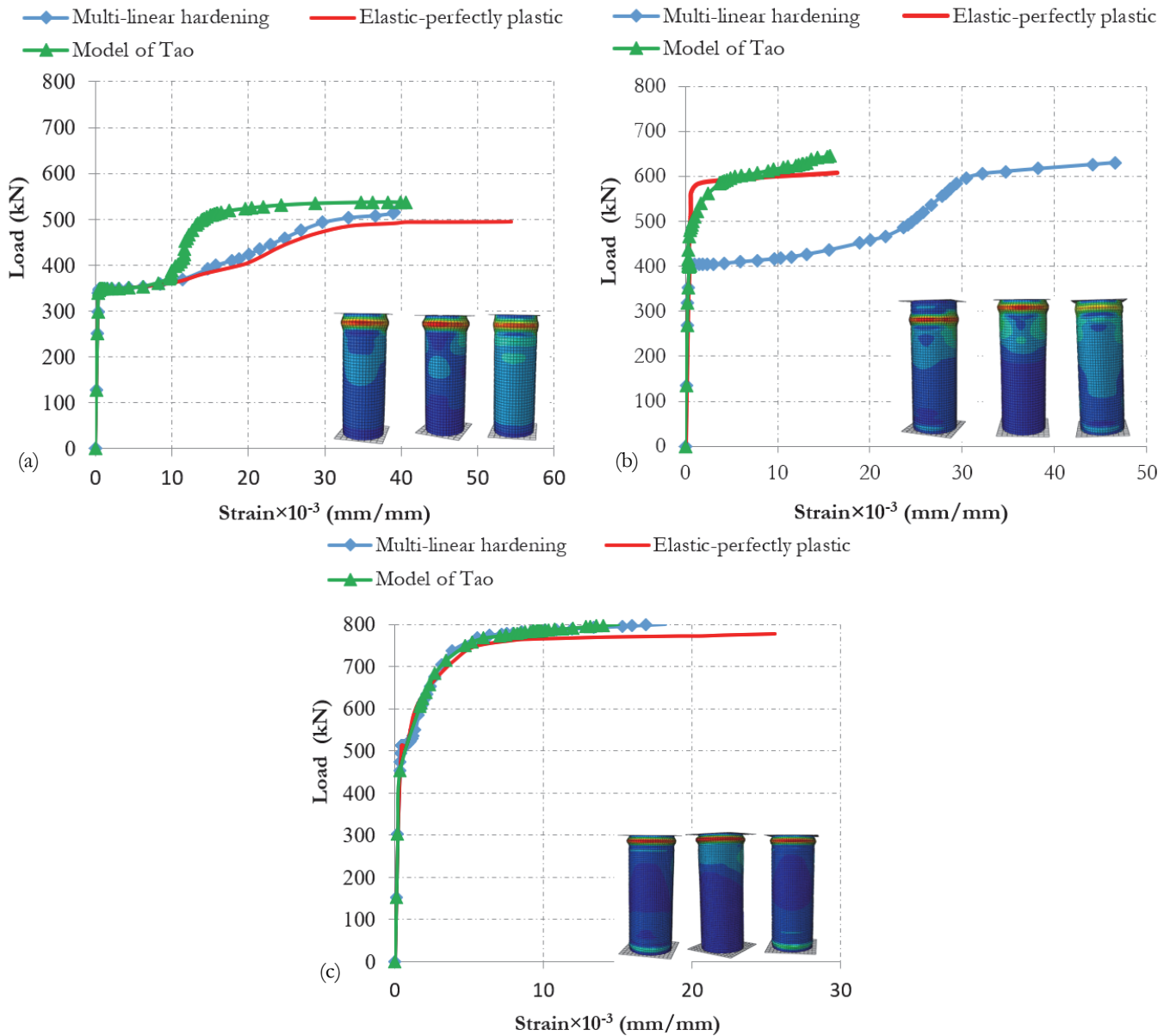


Figure 9: Lateral load-deformation state under different plastic state behaviors (a) T1C3 tube, (b) T2C3 tube, and (c) T3C3 tube.

Regarding the behavior of the model in perfect elasto-plastic state, we note a plastic flow of the short steel tube, with a reduction of the deformation between the tubes T1C3 and T2C3 of about 69% (Figs 9a and 9b). The T3C3 tube modelled by the theory proposed by Tao, presents a buckling at the ends of the short tube, which has been observed by many authors [3,10,24].

Fig. 10 shows the lateral (LE11) and vertical (LE33) deformation state of T2 and T3 tubes successively filled with C1, C2 and C3 type concrete under elasto-plastic behavior with confined concrete proposed by Tao et al [12]. The lateral deformations (LE11) are due to the traction generated by the concrete confined by the steel tube; on the other hand, the vertical deformations (LE33) are compression deformations due to the axial compression.

The curves follow a nonlinear elasto-plastic behavior with the highest value of lateral deformation corresponding to the T3C3 tube reaching  $25 \times 10^{-3}$ , with a local buckling at its ends.

The majority of the vertical deformations (of compression) present a plastic flow with large deformations reaching an average of  $30 \times 10^{-3}$ ; we notice however that the tubes T3C1 and T3C2, gave lateral and vertical deformations of the same order.

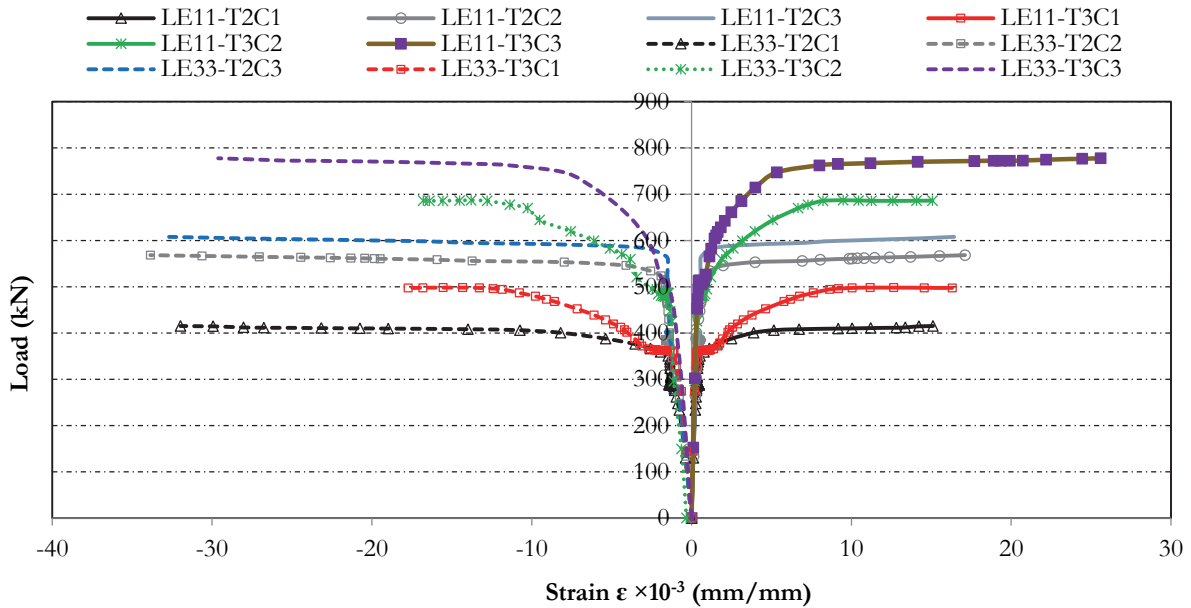
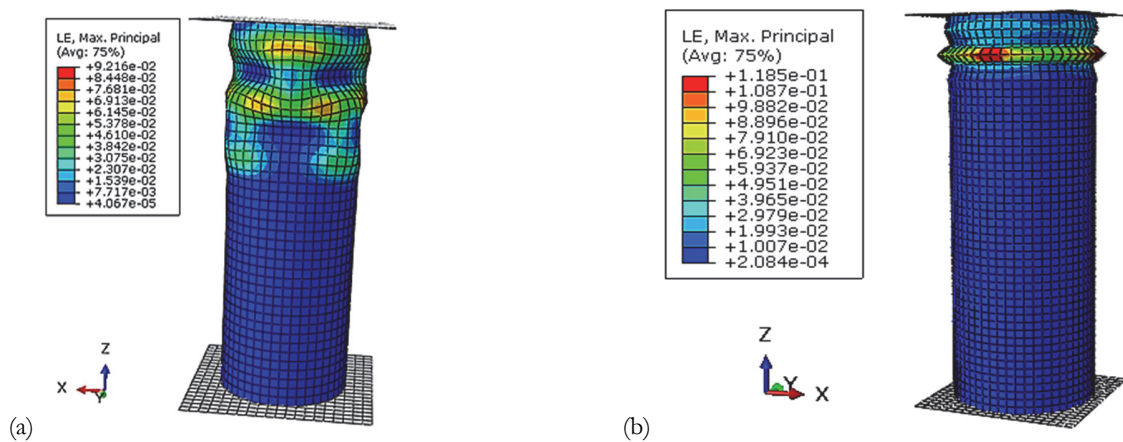


Figure 10: Lateral and vertical deformation state of short tubes T2 and T3 according to the model proposed by Tao et al [12] for confined concrete.

Fig.11 shows the FE failure modes of empty steel tubes ( $f_c = 240$  MPa) in the elasto-plastic state with multilinear hardening (tubes T1, T2 and T3) for which an instability appears in the three tubes with an important blistering on the periphery of the tube T1 (shortest tube) which increases until the middle of the tube, on the other hand we do not observe any buckling in its lower part.



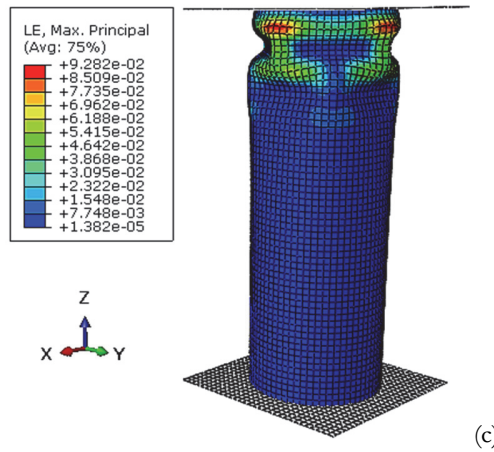


Figure 11: FE failure modes of empty steel tubes ( $f_c = 240$  MPa) in elasto-plastic state with multilinear strain hardening, (a) Tube T1, (b) Tube T2, and (c) Tube T3.

Concerning the failure modes of steel tubes filled with concrete according to the theory of confined concrete T1C1, T2C1 and T3C1, we notice a significant improvement of their behavior under axial compression with a decrease of the maximum deformations, due to the action of the concrete of strength  $f_c = 15$  MPa confined by the tube, but the presence of a slight local buckling, located at the upper end of the tubes.

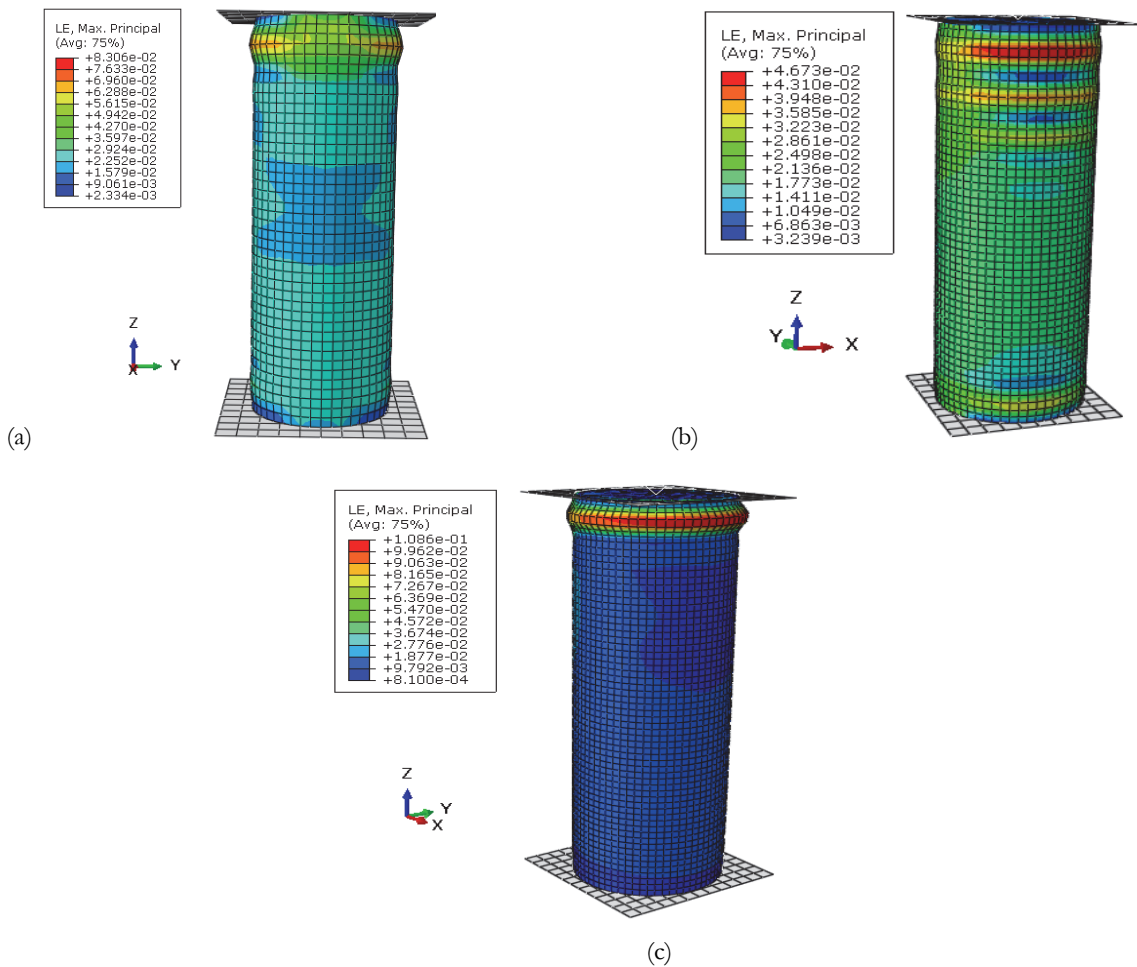


Figure 12: FE failure modes of concrete-filled steel tubes according to the confined concrete theory, (a) T1C1 tube, (b) T2C1 tube, and (c) T3C1 tube.

According to Tab. 3 in which, we have established the theoretical, experimental and numerical results of short tubes filled with concrete, we observe a very good correlation between the values obtained for critical loads that do not exceed 10%.

Models	$P_{\text{Theoretical}}$ $P_{\text{Theo E4}} \text{ (kN)}$	$P_{\text{Numerical}}$ $P_{\text{Num}} \text{ (kN)}$	$P_{\text{Experimental}}$ $P_{\text{Exp}} \text{ (kN)}$	$P_{\text{Theo E4}} / P_{\text{Exp}}$	$P_{\text{Num}} / P_{\text{Exp}}$
T1C1	299.7	315	325	0.92	0.97
T1C2	331.87	318	340	0.98	0.94
T1C3	354.39	338	355	1.00	0.95
T2C1	427.69	417	420	1.02	0.99
T2C2	480.5	425	470	1.02	0.90
T2C3	517.47	500	500	1.03	1.00
T3C1	543.51	500	545	1.00	0.92
T3C2	622.05	600	620	1.00	0.97
T3C3	677.03	700	705	0.96	0.99

Table 3: Results comparison of theoretical, experimental and numerical critical loads of short tubes filled with concrete.

The numerical model with perfect elastoplastic behavior gives a realistic representation in agreement with the experimental and theoretical models.

The histogram in Fig. 13 shows the numerical, theoretical and experimental critical loads of the treated tubes. A very good correlation between the results is observed. Tube T3c3 shows the value of the maximum critical load, which reaches a value of about 700 kN. The T3c3 tube shows larger dimensions and mechanical characteristics compared to other models. Tubes t1c1, t1c2 and t1c3 show an approximate critical load of 310 kN. According to these all results, one can conclude that numerical modelling is reliable for this kind of problem where the difference between the results does not exceed the 5%.

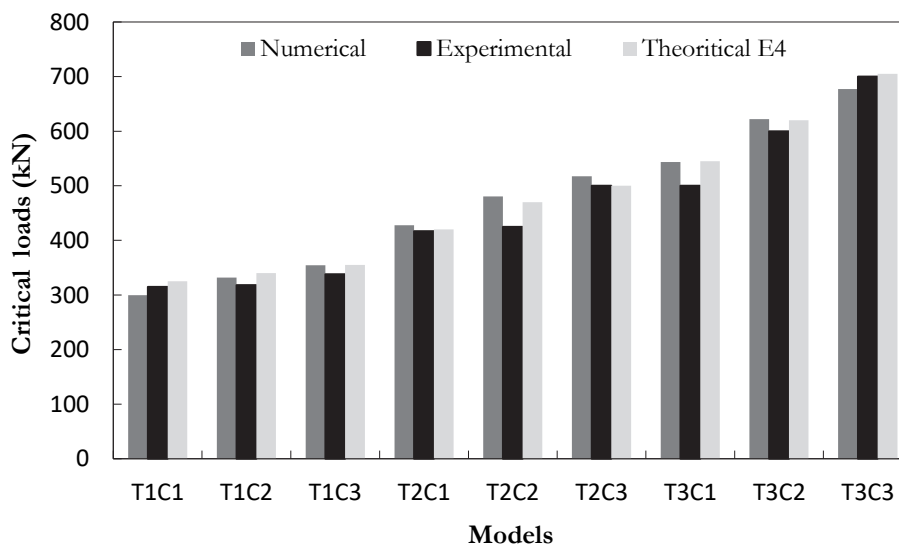


Figure 13: Critical load State of tubes filled with concrete (theoretical Eurocode 4, experimental and numerical).

## CONCLUSION

The material nonlinear numerical modelling of short filled steel tubes, based on the theory of plasticity (perfect elasto-plasticity, elasto-plasticity behavior with multilinear strain hardening and elasto-plasticity with strain hardening proposed by Tao et al [12], allowed us to show the real behavior of short CFST. The validation of the models was carried out in relation to the European Eurocode 4 standards [8] as well as an experimental study and led us to the following conclusions:

- The reinforcement of empty tubes with concrete led to a significant improvement of their load-deformation state.





- For a steel tube filled with concrete (CFST), under axial compression, the concrete core expands laterally and is confined by the steel tube, this confinement is passive in nature and can increase the strength and ductility of concrete.
- The appearance of a local buckling for all the modeled tubes, located in the majority of the cases, at the upper end of the tube, except for certain tubes for which the local buckling appeared at the median part for (T1C2) and at both ends for (T3C3).
- We also notice a very good correlation between the experimental, theoretical, and numerical results with in some cases, a small difference that does not exceed 10%.
- The numerical model with perfect elasto-plastic behavior gives a behavior very close to reality compared to the experimental tests.
- The T3C1 and T3C2 tubes show similar failure modes for the different behavior laws, which leads us to assume that the variation of the plasticity behavior laws does not influence the behavior of the model, but we can assume that the improvement of the material characteristics can have a positive effect, i.e. a decrease of the deformations.

## NOMENCLATURE

$\sigma$ :	Stress
$\epsilon$ :	Strain
$f_u$ :	Ultimate strength
$\epsilon_y$ :	Yield strain
$\epsilon_p$ :	Ultimate strain corresponding to the ultimate strength
$p$ :	Strain hardening exponent
$E_p$ :	Strain hardening modulus of steel
$f_u$ :	Ultimate strength
$E_s$ :	Modulus of elasticity of steel
$f_{ck}$ :	Unconfined compressive cylinder strength of concrete
$f_{ck, cub}$ :	Unconfined compressive cube strength of concrete
$f_{\alpha}$ :	Maximum confined concrete strength
$\epsilon_{\alpha}$ :	Peak strain of confined concrete
$D$ :	External diameter of the tube section
$t$ :	Tube thickness
$f_y$ :	Yield strength of the steel section
$f_l$ :	Confining pressure
$E_{cc}$ :	Initial Young's modulus of the confined concrete
$k_1, k_2, k_3$ :	Coefficients for confined concrete
$R_E, R, R_{\sigma}, R_{\epsilon}$ :	Coefficients for confined concrete

## ACKNOWLEDGMENTS

The authors would like to thank Civil Engineering laboratory - LGC staff of Badji Mokhtar Annaba University (Annaba, Algeria) who provided facilities for conducting the various tests in the laboratory.



## REFERENCES

- [1] Tomii, M., Sakino, K. (1979). Experimental studies on concrete filled square steel tubular beam-columns subjected to monotonic shearing force and constant axial force, *Trans. Archit. Inst. Japan*, 281, pp. 81–92.
- [2] Zeghiche, J., Chaoui, K. (2005). An experimental behaviour of concrete-filled steel tubular columns, *J. Constr. Steel Res.*, 61(1), pp. 53–66.
- [3] Giakoumelis, G., Lam, D. (2004). Axial capacity of circular concrete-filled tube columns, *J. Constr. Steel Res.*, 60(7), pp. 1049–1068.
- [4] Baig, M.N., Fan, J., Nie, J. (2006). Strength of concrete filled steel tubular columns, *Tsinghua Sci. Technol.*, 11(6), pp. 657–66.
- [5] Boursas, F., Boutagouga, D. (2021). Parametric study of I-shaped shear connectors with different orientations in push-out test, *Frat. Ed Integrità Strutt.*, 15(57), pp. 24–39, DOI: 10.3221/IGF-ESIS.57.03.
- [6] Kouider, N., Hadidane, Y., Benzerara, M. (2022). Numerical investigation of the cold-formed I-beams bending strength with different web shapes, *Frat. Ed Integrità Strutt.*, 16(59), pp. 153–171, DOI: 10.3221/IGF-ESIS.59.12.
- [7] Guedaoura, H., Hadidane, Y. (2022). Web post-buckling strength of thin-webbed cellular beams using carbon PFRP profiles, *Frat. Ed Integrità Strutt.*, 16(60), pp. 43–61, DOI: 10.3221/IGF-ESIS.60.04.
- [8] Composite steel and concrete structures - Part 1.1: General rules and rules for buildings Eurocode. (2004). Eurocode 4, CEN (European Committee Stand).
- [9] Hu, H.-T., Huang, C.-S., Wu, M.-H., Wu, Y.-M. (2003). Nonlinear analysis of axially loaded concrete-filled tube columns with confinement effect, *ASCE J. Struct. Eng.*, 129(10), pp. 1322–1329.
- [10] Dai, X., Lam, D. (2010). Numerical modelling of the axial compressive behaviour of short concrete-filled elliptical steel columns, *J. Constr. Steel Res.*, 66(7), pp. 931–942.
- [11] Kebaili, B., Redjel, B. (2012). Etude expérimentale du comportement des tubes en acier remplis de béton, *Eur. J. Environ. Civ. Eng.*, 16(7), pp. 765–776.
- [12] Tao, Z., Uy, B., Liao, F.-Y., Han, L.-H. (2011). Nonlinear analysis of concrete-filled square stainless steel stub columns under axial compression, *J. Constr. Steel Res.*, 67(11), pp. 1719–1732.
- [13] Goel, T., Tiwary, A.K. (2018). Finite element modeling of circular concrete filled steel tube (CFST), *Indian J. Sci. Technol.*, 11(34), pp. 1–9.
- [14] Fang, C., Theofanous, M., Gardner, L. (2013). Numerical modelling of concrete-filled elliptical hollow section columns at ambient temperature. *Proceedings of the Workshop on Finite Element Modelling of Innovative Concrete-filled Tubular Columns under Room and Elevated Temperatures*.
- [15] Jamaluddin, N., Lam, D., Ye, D. (2009). Finite element analysis of elliptical hollow and concrete filled tube columns, *Int. J. Integr. Eng.*, 1(2), pp. 95–101.
- [16] Kedziora, S., Anwaar, M.O. (2019). Concrete-filled steel tubular (CFTS) columns subjected to eccentric compressive load. *AIP conference proceedings*, 2060, p. 20004.
- [17] Mander, J.B., Priestley, M.J.N., Park, R. (1988). Theoretical stress-strain model for confined concrete, *J. Struct. Eng.*, 114(8), pp. 1804–1826.
- [18] Ellobody, E., Young, B., Lam, D. (2006). Behaviour of normal and high strength concrete-filled compact steel tube circular stub columns, *J. Constr. Steel Res.*, 62(7), pp. 706–715.
- [19] Ellobody, E., Young, B. (2006). Nonlinear analysis of concrete-filled steel SHS and RHS columns, *Thin-Walled Struct.*, 44(8), pp. 919–930.
- [20] Richart, F.E., Brandtzaeg, A., Brown, R.L. (1928). A study of the failure of concrete under combined compressive stresses, University of Illinois at Urbana Champaign, College of Engineering. Engineering Experiment Station.
- [21] Seon-Hu, K., Cheol-Ho, L. (2021). Chord sidewall failure of RHS X-Joints in compression and associated design recommendations, *J. Struct. Eng.*, 147(8), pp. 04021111, DOI: [https://doi.org/10.1061/\(ASCE\)ST.1943-541X.0003068](https://doi.org/10.1061/(ASCE)ST.1943-541X.0003068).
- [22] Eurocode 3. (2003). Design of steel structures, Part 1.3 Gen. Rules Supplementary Cold Form. Thin Gauge Members Sheeting, CEN (European Committee Stand).
- [23] Duval, A., Al-akhras, H., Maurin, F., Elguedj, T., Duval, A., Al-akhras, H., Maurin, F., Elguedj, T. (2014). *Abaqus/CAE 6.14 user's manual*, Dassault Systèmes Inc.
- [24] Gupta, P.K., Singh, H. (2014). Numerical study of confinement in short concrete filled steel tube columns, *Lat. Am. J. Solids Struct.*, 11(8), pp. 1445–1462.